Developing a distributed acoustic sensing seismic land streamer: Concept and validation

Adesh Pandey, Jeffrey Shragge, Derrick Chambers & Aaron J. Girard
Center for Wave Phenomena and Dept. of Geophysics, Colorado School of Mines, Golden CO 80401
email: apandey@mines.edu

ABSTRACT
Motivated by existing cabled seismic land-streamer designs, we develop a distributed acoustic sensing (DAS) land-streamer system for high-resolution near-surface seismic data acquisition. The system consists of a DAS interrogator unit (IU), fiber optic cable attached beneath a fire-hose assembly for environmental isolation and improved fiber-ground coupling, and a vehicle-mounted accelerated weight-drop source. The DAS land streamer is easily deployed and towed along the ground surface, allowing for spatially dense data acquisition. We present two field tests with the developed hardware to evaluate the DAS land-streamer performance. The first test investigates the effects of hose weight on the surface-deployed fiber and shows that this approach improves fiber-ground coupling and leads to improved signal-to-noise ratio (SNR). The second test demonstrates that the DAS land streamer records waveforms with similar phase and moveouts as those recorded by horizontal geophones, but offers a higher native spatial density advantage than standard geophone arrays, leading to spatially dense waveforms, improved SNR after post-processing, and superior surface-wave acquisition. Our findings suggest that a DAS land streamer is a promising alternative to traditional geophone-based surveys and may offer several advantages including faster survey acquisition speed and lower field costs due to reduced acquisition hardware requirements. However, methodological limitations include recording a single horizontal ground-motion component, a dependence on favorable fiber-ground coupling conditions, and the upfront cost of IU procurement. A DAS land streamer may be useful in numerous subsurface applications, including multi-channel analysis of surface waves (MASW) or surface-wave inversion for geophysical, geological, geotechnical, and environmental investigations.

Key words: Distributed Acoustic Sensing, Near-Surface Seismic Acquisition

1 INTRODUCTION

Near-surface seismic methods are useful for detecting and characterizing geohazards (Tran and Sperry, 2018; Jiang et al., 2020), evaluating infrastructure (Martínez and Mendoza, 2011), undertaking geological mapping (Inazaki et al., 2001), as well as numerous other applications. Periodic seismic monitoring is used to examine infrastructure health over calendar time and effectively serves as an early-warning system against structural deterioration and potential catastrophic failure. High-resolution seismic surveys are commonly used to image shallow subsurface features in geological, engineering, and environmental investigations (e.g., Miller and Steeples, 1994; Al-Anezi, 2015; Sun et al., 2022). However, a common feature of these surveys is that they require densely spaced sources and receivers distributed over generally short acquisition spreads, resulting in time-consuming (and therefore expensive) manual planting of geophones and frequent movement of acquisition cable spreads.

Over the past decades, the aforementioned survey inefficiencies motivated the development of seismic "land-streamer" systems (van der Veen and Green, 1998) comprised of a towable geophone array connected through a cabling assembly to an seismograph acquisition system. Seismic land streamers have been used for data acquisition in urban areas to address a variety of subsurface

challenges. Inazaki (1999) and van der Veen et al. (2001) developed and successfully applied towed land-streamer systems for high-resolution shallow shear-wave reflection surveying. Ivanov et al. (2006) and Inazaki and Nakanishi (2009) used similar systems for detailed near-surface fault imaging while Inazaki et al. (2005) applied a similar methodology for near-surface cavity and tunnel detection. Suarez and Stewart (2008) and Hanafy (2022) compared field data sets from conventional near-surface geophone and land-streamer setups and found that the data sets are of comparable quality.

While the geophone-based land streamers demonstrably save acquisition time and can provide data of similar quality to traditional acquisition techniques, they are limited by the maximum towable length due to the weight and bulk of associated instrumentation (e.g., geophones, digitizers) and signal communication cabling. This, in turn, limits the available channel count and sensor density, which adversely affects spatial resolution. Additionally, the sometimes poor geophone-ground coupling can lead to suboptimal signal-to-noise ratio (SNR).

Distributed acoustic sensing (DAS) offers a relatively new modality for near-surface seismic acquisition. DAS interrogator units (IUs) transform lightweight fiber optic cables into a dense array of seismic sensors and allow for deployments with sub-meter spatial and kiloHertz (kHz) temporal sampling (Parker et al., 2014). DAS is used in various seismic imaging applications including natural hazard detection (Hudson et al., 2021), natural resource exploration (He et al., 2022; Martuganova et al., 2022), and urban structural health monitoring (Yuan et al., 2021). Mestayer et al. (2011), Mateeva et al. (2012), and Correa et al. (2017) demonstrated that DAS vertical seismic profiling (VSP) surveys have potential to provide similar - or even superior - quality data sets compared to VSP conventional geophone acquisition. Fernández-Ruiz et al. (2020) showed the promising performance of low-frequency ($<$1 Hz) DAS recording when compared to broadband seismometers. However, most favorable comparisons between geophone and DAS-based acquisition are made with permanent and downhole fiber installations, which enable near-perfect elastic coupling to the surrounding earth. Obtaining favorable matches between geophone and DAS data acquired using temporary surface deployments of horizontal fiber remains technically challenging due to the often-poor fiber-ground coupling and the associated loss in data quality. Nonetheless, Spikes et al. (2019) demonstrated that DAS with helically wound cables can acquire near-surface reflection seismic data comparable to conventional geophones when laying fiber cables on the surface. Similarly, Mjehovich et al. (2023) showed that adequate sensitivity to dynamic strain can be achieved in stationary rapid surface deployments of DAS fiber under self-gravity fiber-ground coupling conditions.

Given the limitations of cabled geophone systems and the growing prominence of DAS technology, we posit that a next-generation DAS land streamer can be designed to acquire usable seismic data with natively high spatial sampling rates. The successful development may offer the potential for faster overall survey acquisition speed and smaller field survey crews due to reduction in bulk of associated hardware. However, such a system must overcome key technical challenges, first and foremost being the ability to consistently achieve adequate fiber-ground elastic coupling for rapid horizontal DAS deployment scenarios.

Motivated by the potential for more efficient near-surface seismic investigations, the work presented herein describes the development and testing of a towed DAS land streamer using armored fiber cable weighted down by fire hoses to improve fiber-ground coupling and provide environmental shielding. We first present our overall DAS land-streamer design and some of the key technologies used in its development. We then report the findings of two trial field deployments. The first test investigates the effects of additive hose weight on the fiber and the resulting improvement in fiber-ground coupling. The second test compares seismic waveforms recorded on the DAS land streamer and conventional horizontal geophone acquisition systems in terms of shot-record quality, measured frequency content, and the extracted frequency-velocity dispersion curves. We then conclude with a brief discussion highlighting possible future improvements in the DAS land-streamer acquisition system and our thoughts on the potential implications for geological, geotechnical, and environmental investigations.

2 THEORY

In seismic data acquisition, the term “streamer” typically refers to marine acquisition scenarios where a group of hydrophones is towed behind a vessel and connected to central seismic acquisition units through wiring housed within the towing cable itself. In the land seismic equivalent, a streamer represents an array of geophones designed to be towed along the ground surface. The setup generally includes sturdy cables (van der Veen et al., 2001) or hose (Miller et al., 2003) with an array of takeouts for the geophone units. Individual geophone units consist of spikeless geophones mounted on a housing platform, generally a steel base-plate attached to the towed cable.

Our proposed DAS land streamer represents an extension of conventional seismic land streamers that incorporates DAS-based fiber acquisition technology. Our system tows a weighted fiber cable along the ground surface by an acquisition vehicle, as shown in Figure 1. The tow setup includes a six-strand armored optical fiber cable (manufactured by OCC) attached to multiple sections of fire hose, each 5.1 cm (2.0 in) diameter and 15.2 m (50.0 ft) long, that are connected through standard metallic screw adaptors

and mounted to the acquisition vehicle's trailer hitch or connected to the tow-bar frame. The hose assembly serves two purposes: (1) to weigh down the cable to improve fiber-ground coupling and thereby the quality of recorded waveforms; and (2) to isolate the fiber optic cable from external environmental disturbances, such as wind.

We record DAS land-streamer data using a Treble DAS interrogator unit (IU) from Terra15 Technologies (Perth, Australia). This IU has a broadband recording capability (0.01 Hz to 4.0 kHz) and like other DAS IUs uses the principle of Rayleigh backscattering to effectively turn the fiber optic cable into a sensitive strain gauge (Lindsey and Martin, 2021). When laser pulses are transmitted through the fiber optic cable, they encounter imperfections along its length, which backscatter energy that is measured at the IU to generate a unique "stationary fingerprint" of the fiber at the time of the laser pulse. Seismic waves passing through the ground to which the fiber is elastically coupled measurably strain the fiber, leading to changes in the fingerprint pattern that can be processed to generate seismic-like data through a process analogous to a distributed interferometry system.

The Terra15 Treble IU uses a novel optical measurement design that acquires a "deformation-rate" quantity (Frisken et al., 2019) rather than the strain-rate value typical of other interrogators. Under idealistic fiber-ground elastic coupling conditions (Sidenko et al., 2020), this unique measurement is theoretically equivalent to the single component of ground particle velocity oriented along the fiber axis direction. The measured quantity,

$$\tilde{v}(x,t) = \int_0^x \dot{\epsilon}(u,t)\,\mathrm{d}u, \tag{1}$$

effectively represents the integral of the strain rate $\dot{\epsilon}$ from the interrogation point (at u = 0) to point $u = x$ on the fiber, where t and u respectively represent time and an auxiliary spatial integration variable, and the tilde symbol on $\tilde{v}$ emphasizes that the measured quantity is only equivalent to the true particle velocity of ground motion when the elastic fiber-ground coupling conditions are met. This native deformation-rate data type enables "gauge-free" operation, meaning that a gauge length (GL) need not be defined at the time of data acquisition. Rather, deformation-rate data can be converted post-acquisition to a strain-rate equivalent using a user-defined GL, which can be as short as 0.8 m in GL-based filters or a selection of other filters (Yang et al., 2022) that provide the equivalent of an along-fiber spatial first derivative (e.g., a high-order finite-difference operator).

Figure 1 illustrates the design and deployment of the developed DAS land streamer for the Test 2 trials described below. Figure 1a shows the fiber cable attached via duct tape to the underside of the hose assembly. The deployed horizontal geophones of the cabled seismic acquisition system are located approximately 1.0 m to the right. Figure 1b shows the R.T. Clark PEG-40 accelerated weight drop source and the DAS land streamer mounted on the towing vehicle. Figure 1c depicts the towed DAS land-streamer system deployed in the field to form a 72.0 m-long streamer.

3 EXPERIMENTS

3.1 Field Test 1: Ground-Fiber coupling

Wave amplitudes and frequencies recorded by seismic instruments are influenced by a variety of factors including the energy spectrum of the source, ground attenuation, instrument-ground coupling, and the frequency response of the acquisition system. For DAS seismic land-streamer surveying, achieving consistently sufficient fiber-ground coupling enables recording ground motion with higher fidelity, whereas poor fiber-ground coupling results in significant amplitude and frequency distortions.

To investigate the effects of the hose weight on fiber-ground coupling, we conducted a field test at a site covering both a compacted gravel parking lot and natural grass-covered sandy-clay soil area. Figure 2a presents a simplified sketch of the experimental survey geometry. We installed two parallel fiber segments separated by less than 0.2 m. Section A was 45.7 m long and taped under three connected hose segments each of 5.1 cm (2.0 in) diameter and 15.2 m (50.0 ft) length and weighing 9.53 kg. Section B was 75.0 m long and left uncovered. We used a 5.0-kg sledgehammer impacting a metal plate as the seismic energy source. For this test, we fixed the streamer and acquired ten shots at 5.0 m intervals, starting from and ending at the two ends of the 45.7-m hose-covered fiber cable. The test recorded 12 GB of continuous DAS data in deformation-rate format at 0.8 m and 2.0 kHz spatial and temporal sampling intervals, respectively. We then converted deformation-rate data to a strain-rate equivalent using a 12th-order finite-difference approximation of the spatial first-derivative operator (Yang et al., 2022).

The three columns of Figure 3 present shot gathers 4, 7, and 10, while the upper and lower rows show the shot gathers recorded on the weighted Section A and uncovered Section B, respectively. The survey geometry corresponding to the two sections is shown at the top of each panel. The red star indicates the shot points, the thicker dark lines represent the hose-weighted fiber sections, and the thinner red lines represent uncovered fiber sections.

Figure 4a and 4c respectively present the hose-weighted and uncovered fiber sections of the shot gather shown in Figure 3b, while Figure 4b and 4d present the associated $f - k$ spectral magnitudes. We observe that the two fiber sections, although they

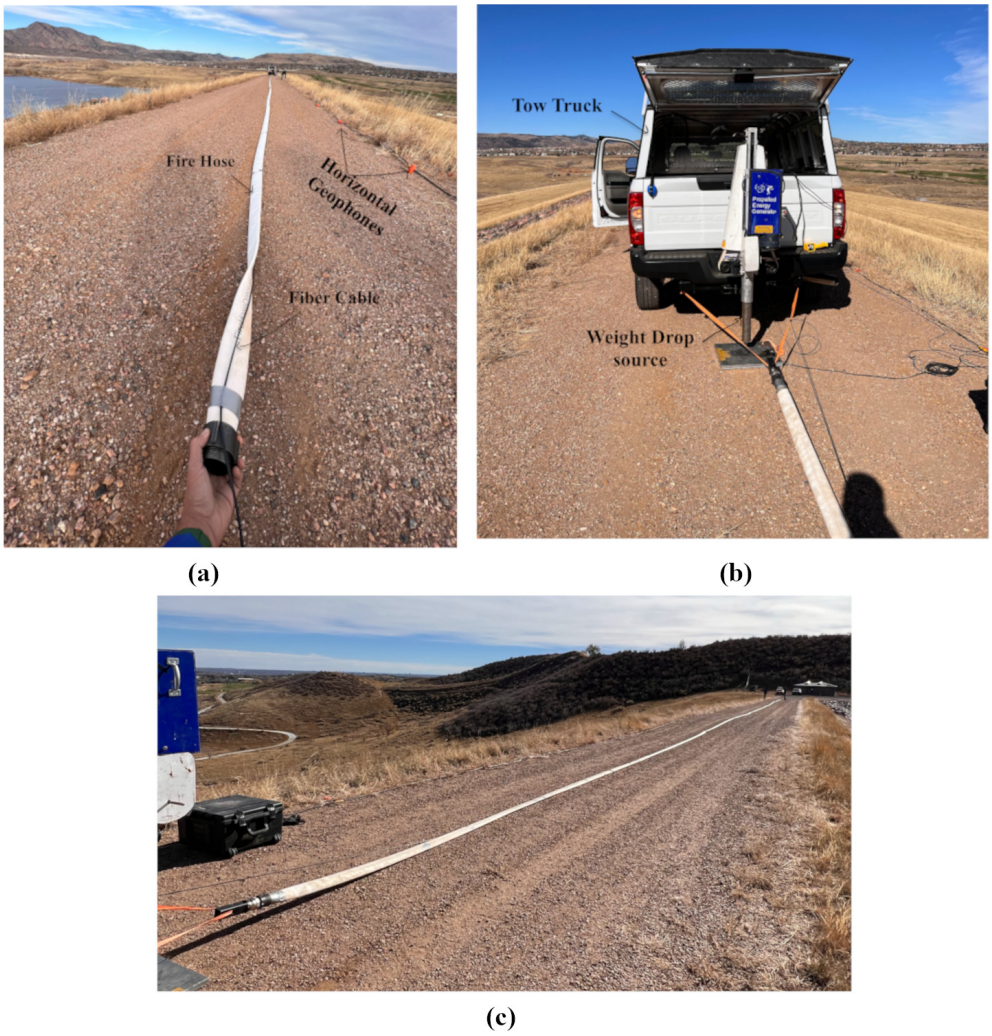

Figure 1. Illustrating the DAS land-streamer design deployed during field Test 2. (a) DAS land-streamer module twisted to show the fiber cable held in place by duct tape to the underside of the hose assembly. Deployed horizontal geophones of the cabled seismic acquisition system are visible approximately 1.0 m to the right. (b) The PEG-40 accelerated weight drop source (R.T. Clark) and DAS land streamer are shown mounted on the acquisition vehicle. (c) The towed DAS land-streamer system in the field with a 72.0 m long streamer.

were separated by only 0.2 m apart, recorded significantly different events (indicated by arrows in Figure 4a and 4c). In particular, the uncovered fiber section (Figure 4c) exhibits high-frequency coherent linear events that travel farther (up to 40 m) and move out faster (approximately 1.8 km/s) than the events recorded in the weighted section. However, these events are not caused by seismic waves propagating through the ground; rather, they are the result of the uncovered and poorly environmentally shielded fiber being disturbed by source energy at the nearby shot location. This energy excites physical waves within the fiber core that propagate with low loss using the fiber as a wave guide and generate coherent noise that masks the expected surface-wave arrivals. In contrast, the data from the hose-weighted section do not exhibit this wave-guide behavior and instead show clearer surface-wave arrivals that diminish in amplitude at farther source-receiver offsets, likely due to local near-surface attenuation. These results suggests that weighting the fiber with a fire hose (or an equivalent system) not only shields the fiber from external disturbances and environmental noise, but also significantly improves ground-fiber coupling.

3.2 Field Test 2: Signal quality tests

The second field test compares the signal quality of the DAS land-streamer data with that of data acquired on conventional horizontal geophones. The test was carried out on a flat 0.5 km gravel-sand section of an earthen embankment located in the western suburbs

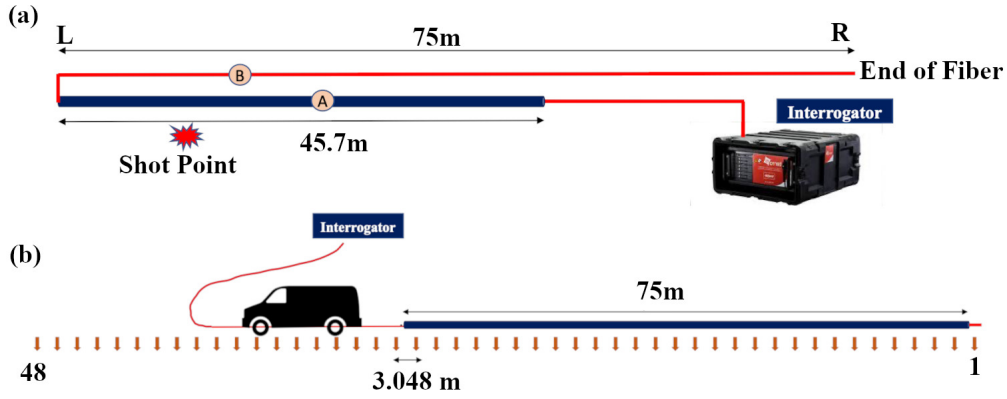

Figure 2. Schematic drawings of DAS acquisition geometry for the two field tests. (a) Hammer seismic test (Test 1) involving a 45.7 m section of fiber corresponding to the fire hose weighted fiber section (labeled A) with a parallel 75.0 m section of uncovered fiber (labeled B), not to scale. The uncovered fiber in section A is connected to the DAS interrogator unit. The shot point shown corresponds to the shot gather presented in Figure 4. (b) The accelerated weight drop test (Test 2) using a 72.0 m streamer section weighted with fire hoses and towed along the survey line with five repeat shots taken at each geophone station between geophones 24 and 48.

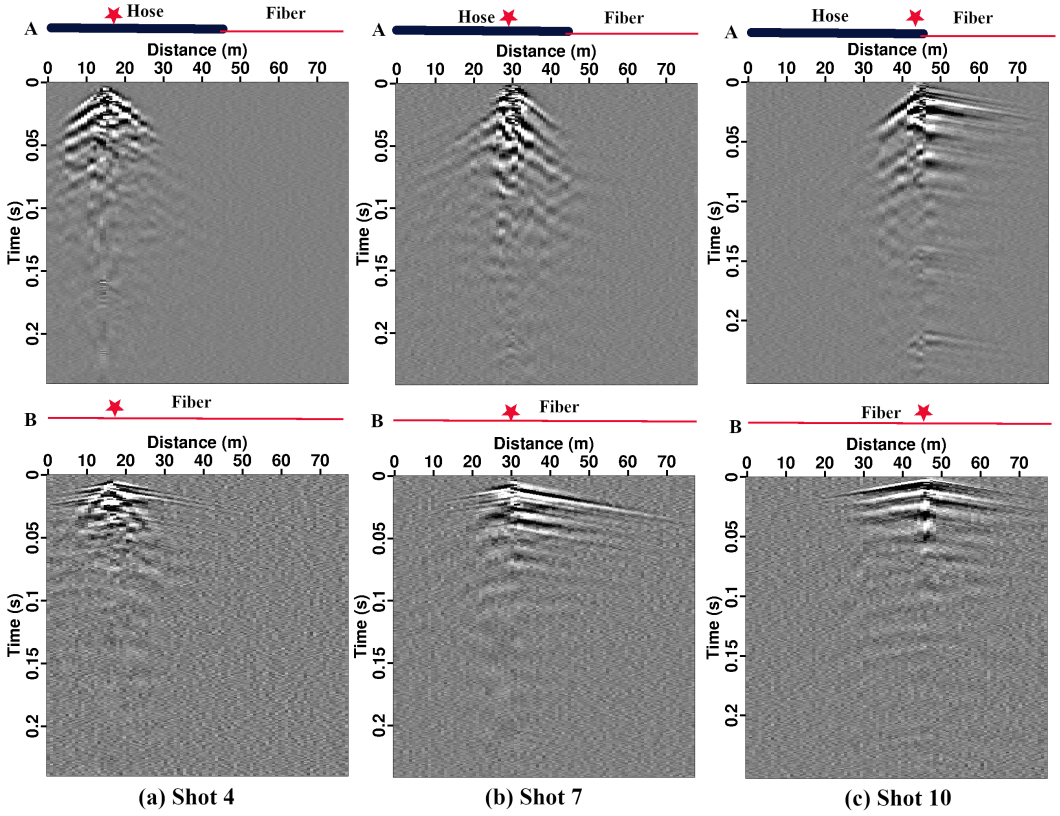

Figure 3. Three representative shot gathers (numbers 4, 7, and 10) from Field Test 1. The top of each panel shows the shot location (red star) and survey geometry corresponding to Sections A (top panels) and B (bottom panels) of Figure 2a. The thicker dark blue lines represent the hose-weighted fiber while the thinner red lines represent the uncovered fiber section.

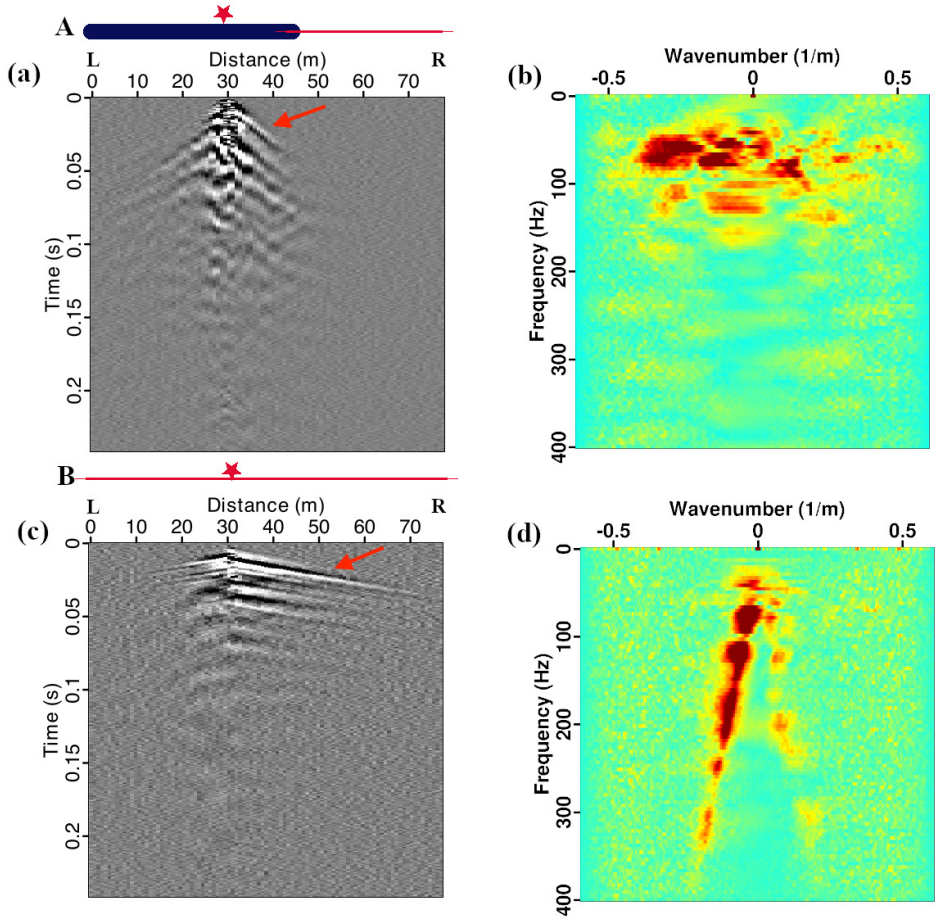

Figure 4. Shot gathers (left panels) and associated $f - k$ spectra (right panels) for Shot 7 presented in Figure 3b. (a-b) Shot gather recorded on the hose-weighted fiber segment in Section A. (c-d) Shot gather recorded on the uncovered fiber segment in Section B. The shot location (red star) and survey geometry are indicated over top of the left panels. The two white arrows indicate the energetic early arrivals referenced in the text.

of Denver, Colorado, USA. We used a 72.0 m fiber streamer cable similarly weighted down by five segments of the same fire hose as in the first test. Figure 1b shows both the survey area and acquisition setup. We also deployed 48 horizontal 10 Hz geophones at 3.048 m (5.0 ft) spacing alongside the land-streamer cable that were oriented parallel to, and offset approximately 1.0 m from, the streamer fiber (Figure 1a). This acquisition geometry allowed for comparative tests with a maximum of 23 geophones overlapping the streamer cable at any given time (see Figure 2b).

We recorded a 200 GB continuous stream of data on the Terra15 IU in the deformation-rate format with 0.8-m and 1.0 kHz spatial and temporal sampling rates, respectively. The geophone signals were recorded using a Geometrics Geode acquisition system also set at a 1.0 kHz sampling rate. Given the greater distances involved in this experiment compared to Test 1, we employed a R.T. Clark PEG40 40 kg accelerated weight drop source to impart more energy in the ground than sledgehammering. The seismic source and DAS land streamer were mounted on an acquisition vehicle via a standard trailer hitch and tow straps (Figure 2b). The IU was situated at the end of the array at a stable base-station location and not deployed in the source vehicle. The DAS land streamer was towed between the 24th and 48th geophone, with shot points located every 3.05 m (10.0 ft). At each of the 25 shot locations, we acquired five repeat weight-drop source strikes for waveform stacking purposes. Because we acquired continuous data records and no trigger was used to determine time zero of shots, we noted approximate shot times for later extraction of shot-gather records from the continuous DAS data stream. Extracting DAS shot gathers reduced the data size from a 200 GB to a more manageable 2 GB data volume. We then used a cross-correlation analysis to determine an optimal set of shot times for the purpose of stacking the DAS shot records from the same source location. The triggered geophone shot records were stacked directly within the Geode cabled acquisition system.

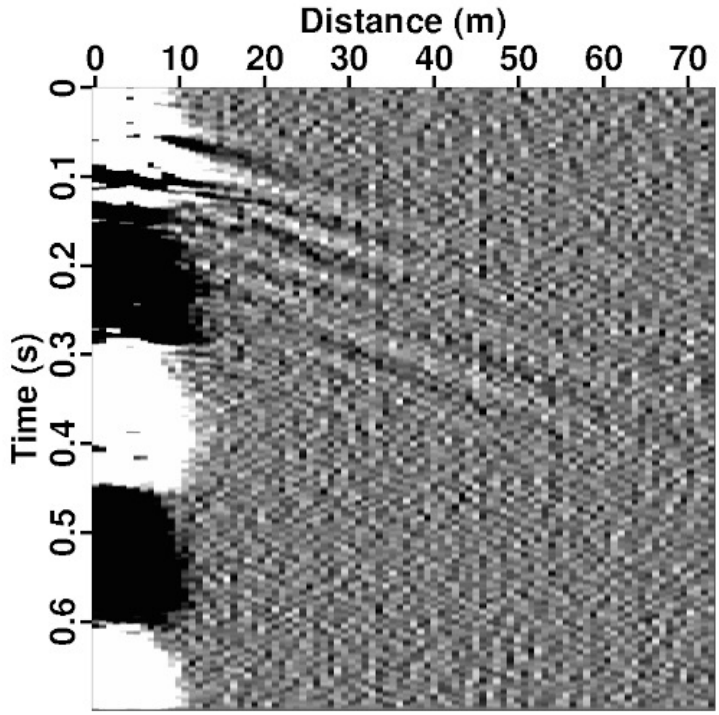

Figure 5. Representative raw DAS shot record from Test 2 showing that the first 15 m of source-receiver offset were largely unusable due to vibrations induced in the fiber by the towing vehicle during accelerated weight-drop acquisition.

Figure 5 illustrates an unexpected acquisition challenge where the first 15 m of source-receiver offset for each shot gather were largely unusable. The cause of this coherent noise source was the starting portion of DAS land streamer being suspended in the air because the towing system (i.e., orange straps shown in Figure 1b and 1c) left too little slack in the tow system for cable to lie completely on the ground. As a result, shot vibrations from the tow vehicle were transferred to the first 15 m of fiber (i.e., approximately to the first metal hose connector). A straightforward solution to this issue would be to roll back the towing vehicle approximately 0.5 m before acquiring a shot so that the straps are loose and the entire streamer is in contact with the ground.

For the purposes of the present experiment, we simply removed the 15 m of unusable data to emphasize the seismic events visible at farther offsets. We then applied a Butterworth band-pass filter between 0.1 Hz and 80.0 Hz to the remaining offsets based on the frequency range of interest for waves generated by the accelerated weight-drop source. We subsequently converted the deformation-rate data to a strain-rate format again using a 12th-order finite-difference approximation of the spatial first-derivative operator (Yang et al., 2022).

Figure 6a and 6b respectively show strain-rate shot gathers and the associated $f-k$ spectra. The observed surface-wave signals are relatively weak compared to the contaminating "salt-and-pepper" noise. To improve the shot-record SNR, we applied iterative trace balancing operation in an $x-t$ window (Fomel, 2007) to reduce the noise and boost signals at farther source-receiver offsets. Figure 6d presents the $f-k$ spectrum of the shot gather shown in Figure 6c where the surface-wave arrivals of interest have apparent velocities (i.e., $V_{app} = \frac{df}{dk}$) between 0.1 km/s and 2.0 km/s.

Because the processed shot-gather data contained residual low-wavenumber and low-frequency noise, we applied a $f-k$ domain velocity-dip mute filter with a pass-band corresponding to the observed 0.1 km/s and 2.0 km/s apparent velocities. The filtered panels were then transformed back into the time-space $t-x$ domain using an inverse 2-D Fourier transform. Figure 6e and 6f presents the resulting shot gather and $f-k$ magnitude spectra after applying the velocity-dip filter. Because the frequencies of interest from the weight-drop source were lower than 45 Hz (Figure 6d), we further applied a 3-40 Hz band-pass filter to the data panels. Overall, this filtering strategy reduced the residual low-wavenumber and low-frequency noise and improved surface-wave arrival continuity. The geophone data were processed using the same workflow as applied to the stacked DAS data.

Figure 7a shows a representative post-processed DAS shot gather. The shot panel is largely consistent in terms of signal continuity and coherency; however, subtle differences in source signatures and amplitudes are visible and are likely due to fiber-

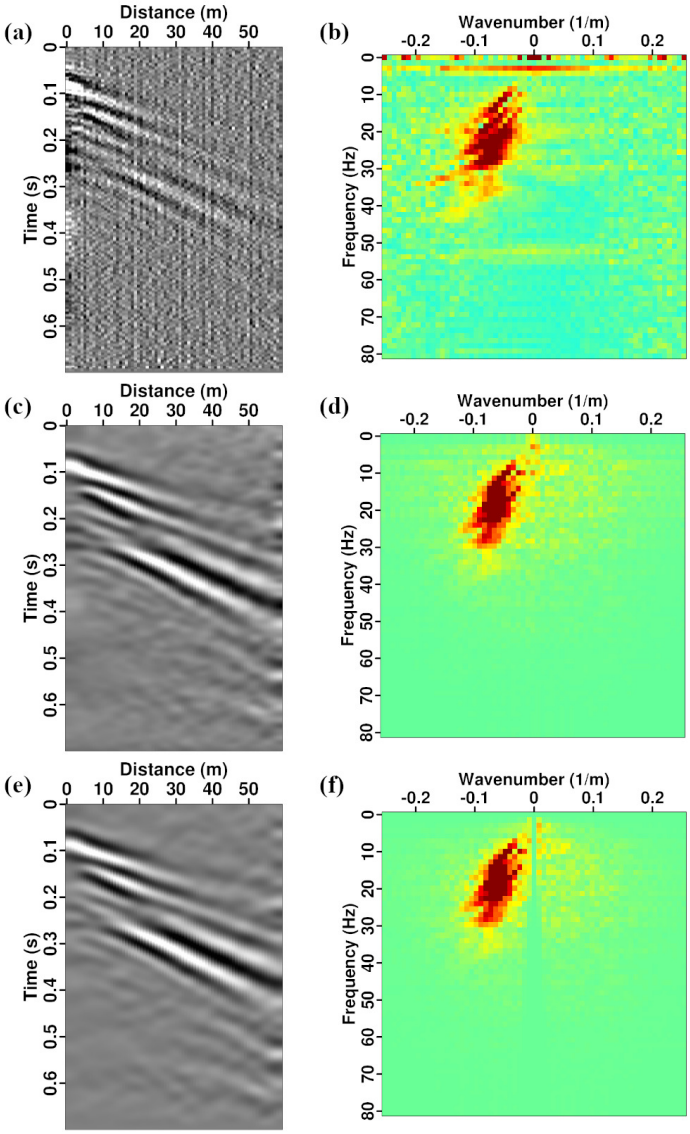

Figure 6. Processing of shot gathers and associated $f - k$ magnitude spectra for Test 2. (a) Strain-rate shot gather panel prior to processing and (b) the associated $f - k$ spectra. (c) Data from (a) after applying the trace balancing and 3-40Hz band-pass filter. (d) corresponding $f - k$ magnitude spectra. (e) Shot gather from (c) after applying velocity-dip filtering corresponding to a pass-band between 0.1 km/s and 2.0 km/s apparent velocities and (f) the associated $f - k$ magnitude spectra.

ground coupling or true localized variations in the near-surface geology. Figure 7b displays the corresponding geophone shot gather to Figure 7a. Figure 7c and 7d show the overlay of geophone data (wiggle plot) on the corresponding DAS shot gather (gray scale). The surface waves recorded from both sensors display comparable arrival phases and apparent moveout velocities.

3.2.1 DAS and Horizontal Geophone Shot Gather Comparison

We next compare the DAS data with the corresponding traces from horizontal geophones that were offset approximately 1.0 m from the land-streamer fiber. Figure 8a-8c respectively present a dense raw shot gather from the DAS land streamer, the corresponding filtered shot gather, and the filtered shot gather subsampled to geophone spacing. Figure 8d and 8e respectively present raw horizontal geophone data corresponding to DAS shot in Figure 8a, followed by filtered geophone shot. We removed three geophone traces due to faulty connections with the data cable.

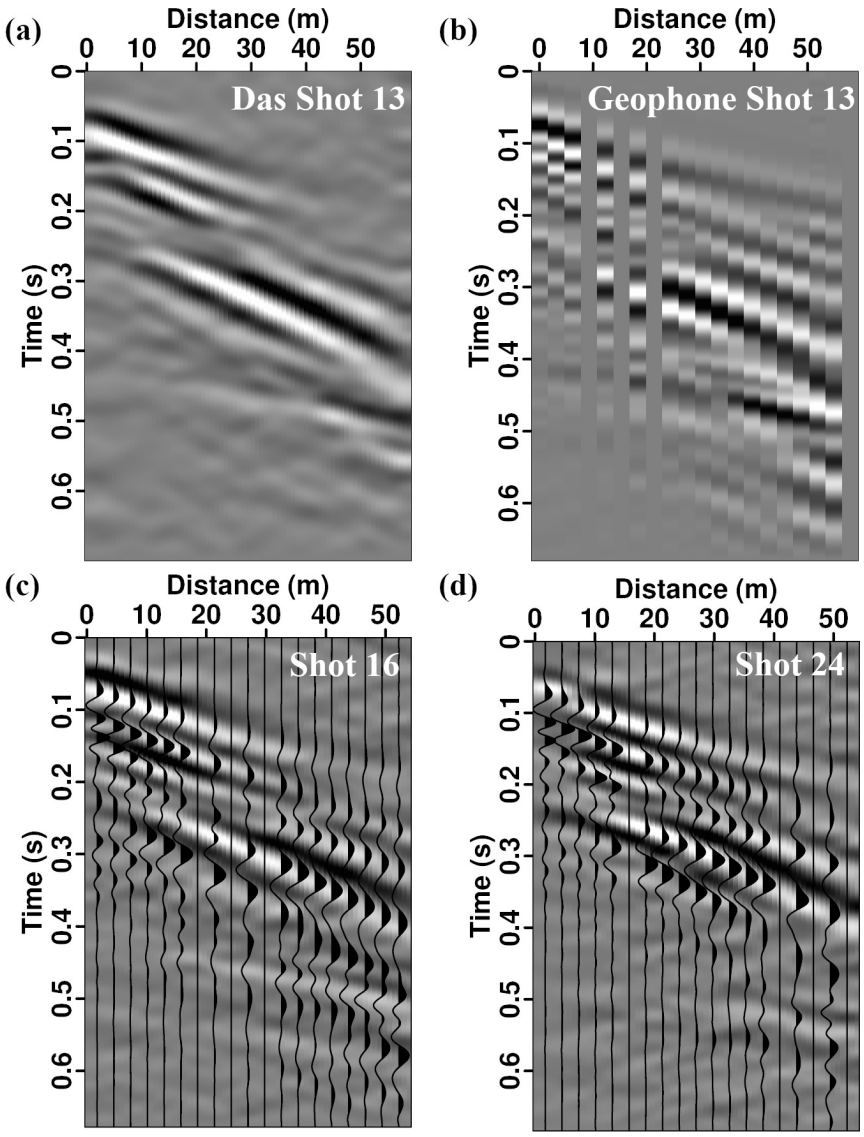

Figure 7. Representative Test 2 shot gathers after post-processing. (a) DAS shot (b) geophone shot corresponding to DAS shot in (a). (c) and (d) DAS (grey) and corresponding geophone shot gather (wiggle) overlays.

The raw DAS shot record exhibits greater levels of noise as compared to raw geophone shot record; however, these effects can be easily removed as outlined above. Compared to the processed geophone records, the dense DAS record (Figure 8b) exhibits improved signal coherency and continuity due to both the natively higher spatial sampling as well as the post-processing workflow enabled by the higher spatial acquisition density. However, the DAS shot record fails to capture very low amplitude far-offset direct arrivals when compared to horizontal geophones. The subsampled DAS record (Figure 8c) demonstrates comparable signal coherency and continuity to the corresponding geophone shot-record (Figure 8e). As demonstrated in Figure 7c and 7d, the surface waves from the two sensor types, though, exhibit similar arrival phases and apparent moveout velocities.

Figure 9c and 9d display frequency-velocity dispersion panels from the processed DAS and geophone shot gathers respectively presented in Figure 9a and 9b. We computed these panels using the phase-shift approach (Park et al., 1998, 1999) as implemented by the open-source MASWaves software package (Ólafsdóttir et al., 2018a,b). The interpreted fundamental Rayleigh wave mode (R0) displays the greatest energy and is more clearly represented in the DAS velocity-frequency dispersion panels. Higher-order wave modes (R1 and R2) also are interpreted to be present in both dispersion panels; however, they are more clearly separated with higher SNR using data from the DAS land-streamer acquisition.

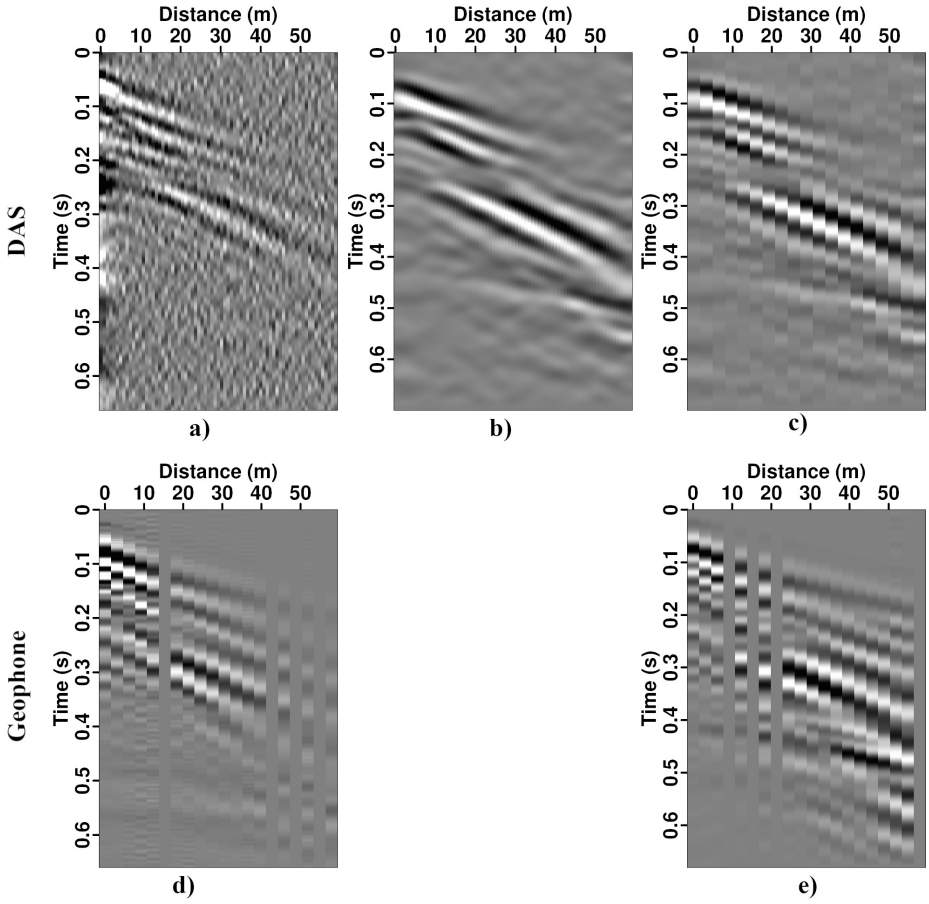

Figure 8. Representative (a) dense raw DAS data. (b) filtered DAS data of (a) (after trace balancing, bandpass, and $f-k$ filtering). (c) horizontally subsampled DAS data of (b). (d) raw horizontal geophone data corresponding to DAS shot in (a). (e) filtered horizontal geophone data of (d) (after similar trace balancing and bandpass as applied to the DAS shot).

Finally, Figure 10 presents the normalized frequency magnitude spectra for combined DAS and geophone shot records. The dominant frequency bands of the DAS (blue) and geophone (red) records are largely similar, but the DAS data appear to have slightly better low-frequency response than geophones, likely due to the relatively rapid roll-off in the sensitivity of the 10 Hz geophones (i.e., 10% sensitivity at 4 Hz). It is worth noting that the PEG-40 accelerated weight drop source used in this test is not designed to generate sub-4.0 Hz energy; however, the DAS system has an improved lower-frequency response compared to that of the geophones and could record such energy if it were available from a different energy source.

4 DISCUSSION

Herein we discuss several DAS land-streamer challenges and considerations that affect data quality and acquisition efficiency. We also present our thoughts on possible DAS land-streamer application use cases.

4.1 Fiber Weighting Considerations

Additional weight on the fiber improves the fiber-ground coupling compared to using the weight of the uncovered fiber alone. While it may be possible to further enhance coupling by filling the hose with a denser material like water or sand, this approach may introduce additional complexities such as generating fluid motion inside the hose due to land-streamer movement, decreased streamer maneuverability, and increased abrasion on the fiber during extended surveying. During the development stages, we tested

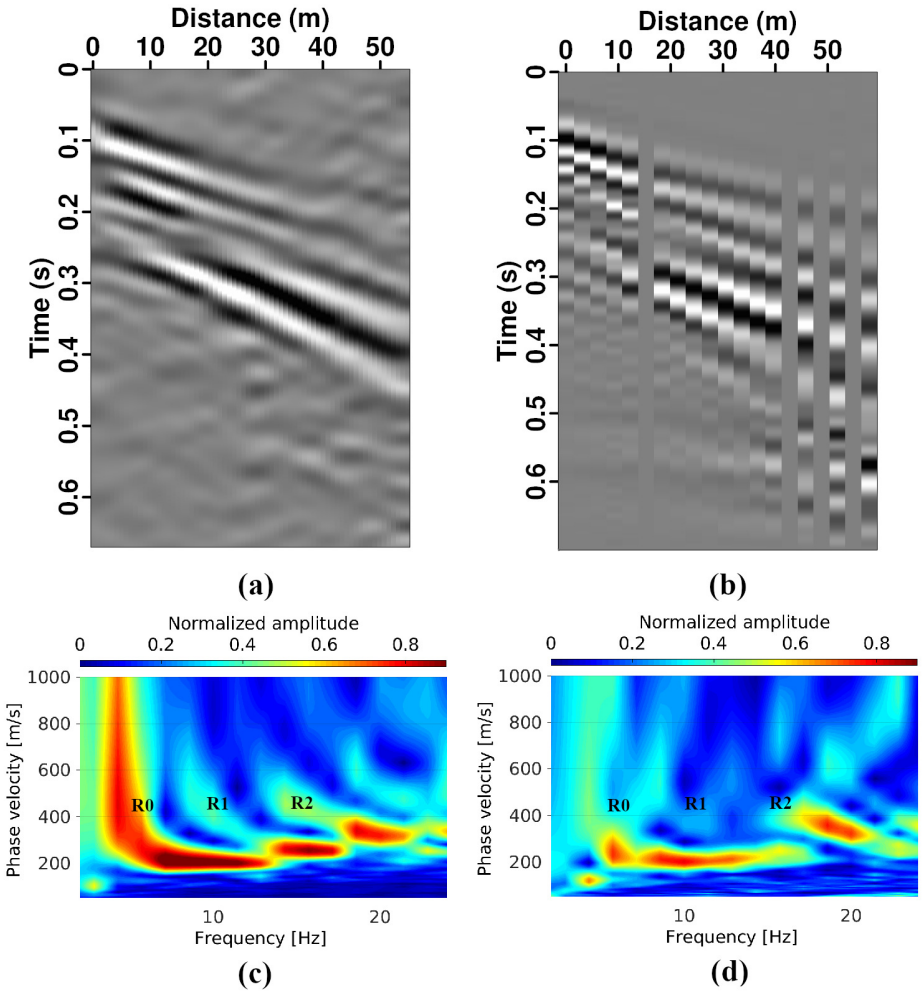

Figure 9. Representative shot gathers recorded on (a) DAS land streamer (after DAS processing) and (b) horizontal-component geophones. (c) Estimated dispersion image corresponding to DAS shot gather in (a). (d) Estimated dispersion image corresponding to DAS shot gather in (b).

a land-streamer design that incorporated a water-filled hose; however, the inclusion of fluids in the hose generated guided waves, which introduced significant amounts of unwanted coherent energy.

The armored fiber cable used in the above experiments is only sensitive to ground motion in the axial direction of the fiber. To improve this directional sensitivity, helically wrapped fiber could be used underneath the hose assembly, which improves sensitivity in the axial and radial directions (Spikes et al., 2019). Additionally, using armored cable heavier than that used in the above tests would likely provide improved self-gravitational coupling.

4.2 IU Location Considerations

Our experiments involved an IU situated at the end of the array at a stable base-station location and not in the source vehicle. Although this effectively isolated the IU from tow-vehicle vibrations, it was less efficient because the fiber cable connecting the streamer to the IU needed to be constantly safeguarded while the tow vehicle moved forward, which was not only time-consuming but required an additional person in the field to safeguard the cable. We point out that the IU could reside in a separate trailing vehicle, which would similarly isolate the IU from shot vibrations and reduce the need for cable management. However, the stability of the internal IU laser for a system mounted in an acquisition vehicle needs further investigation. While this may not pose a problem for flat terrain where the IU remains relatively horizontal, one effect of uneven terrain is it may tilt the IU and introduce laser instabilities that reduce data quality.

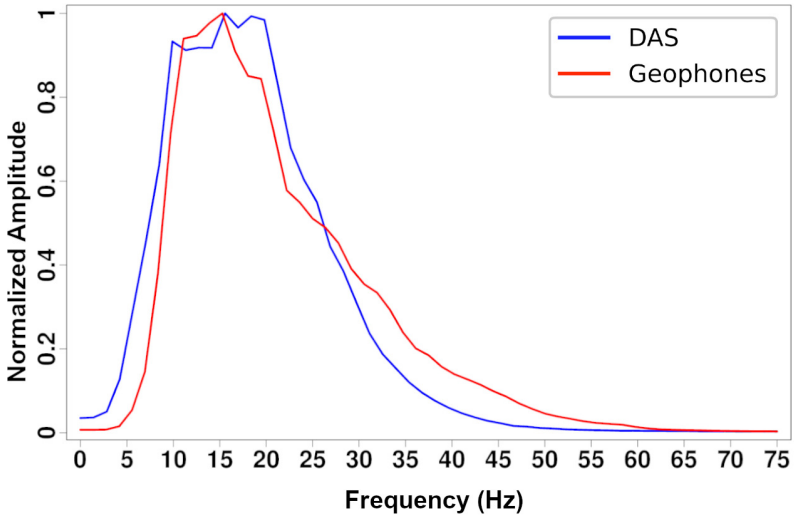

Figure 10. Normalized frequency spectra for the DAS land streamer (blue) and geophone (red) data sets.

4.3 Fiber Array Lengths

Our field tests involving streamers with a 72 m maximum array length (see Figure 5) recorded data with high SNR values to the end of the array (Figure 6). However, many geotechnical surveys require imaging of shallow features to 50 m or even greater depths. Achieving this would require a longer fiber array length between 100-200 m. It would be valuable to test the DAS land streamer with longer segments to determine the operational length limit with the current design. Of course, the effectiveness of an elongated DAS land-streamer design would depend heavily on surface-terrain conditions.

4.4 Vision for DAS land-streamer usage

Based on the described characteristics, we assert that this developed DAS land streamer could be rapidly deployed for active-source seismic surveys in highly favorable surface conditions like compacted soils, earthen embankments, or pavement. This would enable its use in wide range of near-surface seismic characterization applications, including geological mapping, geohazards characterization, environmental monitoring, infrastructure evaluation, and geotechnical engineering investigations. Furthermore, when paired with an autonomous vehicle, a DAS land streamer could also be deployed at difficult-to-access locations including ice sheets, permafrost, glaciers, and sites contaminated by radioactivity.

5 CONCLUSIONS

We present a DAS land-streamer design for near-surface seismic acquisition that represents a promising alternative to traditional geophone-based seismic surveying. The system consists of an acquisition vehicle-towed fiber optic cable that is weighted down by multiple hose segments to improve fiber-ground coupling and provide environmental shielding. Our prototype DAS land streamer acquired seismic waveforms similar to those recorded by sparser horizontal geophone arrays, but in our experience required reduced effort and offered faster acquisition speeds due to lower hardware requirements and ease of tow and roll-along versus rolling a geophone spread. Field trials and our analysis of recorded waveforms suggest that the natively dense spatial sampling capabilities of modern DAS interrogator units and post-processing workflows enable the recording of high-resolution, unaliased surface-wave data (and follow-on analysis products such as velocity-dispersion plots) compared to conventionally acquired sparse geophone array data. While acquiring similar density geophone data can be done using densely spaced geophones, such an acquisition would significantly increase survey time and effort compared to a DAS land streamer. Comparison of the same spatial density DAS and geophone data shows comparable seismic waveforms. However, the effectiveness of the DAS land streamer is strongly dependent on favorable surface conditions for ground-fiber coupling, and there are opportunities for improvements to the design and acquisition procedure. Overall, these findings suggest that DAS land streamer may offer rapid deployment of seismic sensors in a variety of geophysical, geological, geotechnical, and environmental near-surface applications.

6 ACKNOWLEDGEMENTS

We gratefully acknowledge the sponsors of the Mines Center for Wave Phenomena consortium, whose support made this research possible. We thank Justin Rittgers and Dorothy Mwanzia for their assistance with the seismic acquisition efforts, and Ge Jin and Eileen Martin for helpful discussions. The open-source Madagascar software package (www.ahay.org) and DAScore python library (www.github.com/DASDAE/dascore) were used to generate reproducible numerical examples and DAS data visualization, respectively.

REFERENCES

Al-Anezi, G., 2015, Near-Surface Investigation Using High-Resolution Seismic Reflection Techniques: ASEG Extended Abstracts, **2015**.

Correa, J., A. Egorov, K. Tertyshnikov, A. Bona, R. Pevzner, T. Dean, B. Freifeld, and S. Marshall, 2017, Analysis of signal to noise and directivity characteristics of DAS VSP at near and far offsets — A CO2CRC Otway Project data example: The Leading Edge, **36**, no. 12, 994A1–994A7.

Fernández-Ruiz, M. R., M. A. Soto, E. F. Williams, S. Martin-Lopez, Z. Zhan, M. Gonzalez-Herraez, and H. F. Martins, 2020, Distributed acoustic sensing for seismic activity monitoring: APL Photonics, **5**, 030901.

Fomel, S., 2007, Shaping regularization in geophysical estimation problems: Geophysics, **72**, no. 2, R29–R36.

Frisken, S. J., N. Issa, and M. A. F. Roelene, 2019, Distributed optical sensing systems and methods: Australia Patent AU2022203105A.

Hanafy, S. M., 2022, Land-Streamer vs. Conventional Seismic Data for High-Resolution Near-Surface Surveys: Applied Sciences, **12**, no. 2, 584.

He, X.-G., X.-M. Wu, L. Wang, Q.-Y. Liang, L.-J. Gu, F. Liu, H.-L. Lu, Y. Zhang, and M. Zhang, 2022, Distributed optical fiber acoustic sensor for in situ monitoring of marine natural gas hydrates production for the first time in the Shenhu Area, China: China Geology, **5**, 322–329.

Hudson, T. S., A. F. Baird, J. M. Kendall, S. K. Kufner, A. M. Brisbourne, A. M. Smith, A. Butcher, A. Chalari, and A. Clarke, 2021, Distributed Acoustic Sensing (DAS) for Natural Microseismicity Studies: A Case Study From Antarctica: Journal of Geophysical Research: Solid Earth, **126**, e2020JB021493.

Inazaki, T., 1999, Land Streamer: A New System for High-Resolution S-Wave Shallow Reflection Surveys, *in* Symposium on the Application of Geophysics to Engineering and Environmental Problems 1999: Environment and Engineering Geophysical Society, Symposium on the Application of Geophysics to Engineering and Environmental Problems Proceedings, 207–216.

Inazaki, T., S. Kawamura, O. Tazawa, Y. Yamanaka, and N. Kano, 2005, Near-Surface Cavity Detection by High-Resolution Seismic Reflection Methods Using Short-Spacing Type Land Streamer, *in* Symposium on the Application of Geophysics to Engineering and Environmental Problems 2005: Environment and Engineering Geophysical Society, Symposium on the Application of Geophysics to Engineering and Environmental Problems Proceedings, 959–970.

Inazaki, T., N. Kusaka, Y. Ashida, S. Takigawa, and S. Yoshimi, 2001, High-Resolution S-Wave Reflection Survey Using Land Streamer for the Safe Driving of a Shield Tunnel, *in* Symposium on the Application of Geophysics to Engineering and Environmental Problems 2001: Environment and Engineering Geophysical Society, Symposium on the Application of Geophysics to Engineering and Environmental Problems Proceedings, SSI4–SSI4.

Inazaki, T., and T. Nakanishi, 2009, Detailed Imaging of Near-Surface Faulting Structure Using Land Streamer, *in* Symposium on the Application of Geophysics to Engineering and Environmental Problems 2009: Environment and Engineering Geophysical Society, Symposium on the Application of Geophysics to Engineering and Environmental Problems Proceedings, 373–382.

Ivanov, J., R. D. Miller, P. Lacombe, C. D. Johnson, and J. W. Lane, 2006, Delineating a shallow fault zone and dipping bedrock strata using multichannal analysis of surface waves with a land streamer: Geophysics, **71**, no. 5, A39–A42.

Jiang, X., Z. Zhanyuan, H. Chen, M. Deng, Z. Niu, H. Deng, and Z. Zuyin, 2020, Natural dam failure in slope failure mode triggered by seepage: Geomatics, Natural Hazards and Risk, **11**, 698–723.

Lindsey, N. J., and E. R. Martin, 2021, Fiber-optic seismology: Annual Review of Earth and Planetary Sciences, **49**, 309–336.

Martínez, K., and J. A. Mendoza, 2011, Urban seismic site investigations for a new metro in central Copenhagen: Near surface imaging using reflection, refraction and VSP methods: Physics and Chemistry of the Earth, Parts A/B/C, **36**, 1228–1236.

Martuganova, E., M. Stiller, B. Norden, J. Henninges, and C. M. Krawczyk, 2022, 3D deep geothermal reservoir imaging with wireline distributed acoustic sensing in two boreholes: Solid Earth, **13**, 1291–1307.

Mateeva, A., J. Mestayer, B. Cox, D. Kiyashchenko, P. Wills, J. Lopez, S. Grandi, K. Hornman, P. Lumens, A. Franzen, D. Hill,

and J. Roy, 2012, Advances in Distributed Acoustic Sensing (DAS) for VSP, *in* SEG Technical Program Expanded Abstracts 2012: Society of Exploration Geophysicists, SEG Technical Program Expanded Abstracts, 739–744.

Mestayer, J., B. Cox, P. Wills, D. Kiyashchenko, J. Lopez, M. Costello, S. Bourne, G. Ugueto, R. Lupton, G. Solano, D. Hill, and A. Lewis, 2011, Field trials of distributed acoustic sensing for geophysical monitoring, *in* SEG Technical Program Expanded Abstracts 2011: Society of Exploration Geophysicists, SEG Technical Program Expanded Abstracts, 4253–4257.

Miller, R. D., K. G. Park, J. Ivanov, C. B. Park, D. Laflen, and R. F. Ballard, 2003, A 2C Towed Geophone Spread for Variable Surface Conditions, *in* Symposium on the Application of Geophysics to Engineering and Environmental Problems 2003: Environment and Engineering Geophysical Society, Symposium on the Application of Geophysics to Engineering and Environmental Problems Proceedings, 1276–1284.

Miller, R. D., and D. W. Steeples, 1994, Applications of shallow high-resolution seismic reflection to various environmental problems: Journal of Applied Geophysics, **31**, 65–72.

Mjehovich, J., G. Jin, E. Martin, and J. Shragge, 2023, Rapid surface-deployment of das cable for earthquake hazard assessment: Journal of Geotechnical and Geoenvironmental Engineering (in press).

Ólafsdóttir, E. A., B. Bessason, and S. Erlingsson, 2018a, Combination of dispersion curves from MASW measurements: Soil Dynamics and Earthquake Engineering, **113**, 473–487.

Ólafsdóttir, E. A., S. Erlingsson, and B. Bessason, 2018b, Tool for analysis of multichannel analysis of surface waves (MASW) field data and evaluation of shear wave velocity profiles of soils: Canadian Geotechnical Journal, **55**, 217–233.

Park, C. B., R. D. Miller, and J. Xia, 1998, Imaging dispersion curves of surface waves on multi-channel record, *in* SEG Technical Program Expanded Abstracts 1998: Society of Exploration Geophysicists, SEG Technical Program Expanded Abstracts, 1377–1380.

———, 1999, Multichannel analysis of surface waves: Geophysics, **64**, no. 3, 800–808.

Parker, T., S. Shatalin, and M. Farhadiroushan, 2014, Distributed Acoustic Sensing – a new tool for seismic applications: First Break, **32**, no. 2, 61–69.

Sidenko, E., A. Bona, R. Pevzner, N. Issa, and K. Tertyshnikov, 2020, Influence of Interrogators' Design on DAS Directional Sensitivity: European Association of Geoscientists & Engineers, **2020**, no. 1, 1–5.

Spikes, K. T., N. Tisato, T. E. Hess, and J. W. Holt, 2019, Comparison of geophone and surface-deployed distributed acoustic sensing seismic data: Geophysics, **84**, no. 2, A25–A29.

Suarez, G. M., and R. R. Stewart, 2008, A field comparison of 3C land streamer versus planted geophone data, *in* SEG Technical Program Expanded Abstracts 2008: Society of Exploration Geophysicists, SEG Technical Program Expanded Abstracts, 16–20.

Sun, R., A. Kaslilar, and C. Juhlin, 2022, High resolution seismic reflection PP and PS imaging of the bedrock surface below glacial deposits in Marsta, Sweden: Journal of Applied Geophysics, **198**, 104572.

Tran, K. T., and J. Sperry, 2018, Application of 2D full-waveform tomography on land-streamer data for assessment of roadway subsidence: Geophysics, **83**, no. 3, EN1–EN11.

van der Veen, M., and A. G. Green, 1998, Land streamer for shallow seismic data acquisition: Evaluation of gimbal-mounted geophones: Geophysics, **63**, no. 4, 1408–1413.

van der Veen, M., R. Spitzer, A. G. Green, and P. Wild, 2001, Design and application of a towed land-streamer system for cost-effective 2-D and pseudo-3-D shallow seismic data acquisition: Geophysics, **66**, no. 2, 482–500.

Yang, J., J. Shragge, and G. Jin, 2022, Filtering Strategies for Deformation-Rate Distributed Acoustic Sensing: Sensors, **22**, 8777.

Yuan, S., J. Liu, H. Young Noh, and B. Biondi, 2021, Urban system monitoring using combined vehicle onboard sensing and roadside distributed acoustic sensing, *in* First International Meeting for Applied Geoscience & Energy Expanded Abstracts: Society of Exploration Geophysicists, SEG Technical Program Expanded Abstracts, 3235–3239.